Journal of Scientific & Industrial Research
Vol. 66, January 2007, pp 37-46

Influences of feed and condenser temperature on molecular distillation of ideal binary mixtures

P Shao[1], S T Jiang[1,2,*] and Y K Ye[1]

[1]School of Biotechnology and Food Engineering, Hefei University of Technology, Hefei 230 009, China

[2]Key Laboratory of Agricultural Production Biochemistry of the Ministry of Education, Hefei 230 069, China

Received 10 January 2006; accepted 17 August 2006

Balanced equations of a binary mixture for molecular distillation (MD) were derived on the basis of relation of heat and mass transfer in liquid films on both the evaporating and condensing surface. Effects of feed temperature and condenser temperature on film thickness, film surface temperature and concentration, degree of evaporation and concentration of distillate were analyzed for MD. The length of evaporating cylinder along with surface temperature of evaporating film reached steady state decreasing with increasing of feed temperature. Evaporation rate decreased with increasing of condenser temperature because of re-evaporation. Influences of splashing on distillate and re-evaporation were minimized and gradient concentration of distillate and increased degree of evaporation were obtained by the divided evaporator and condenser. Evaporating film temperature was increased with the gradient increase of divided evaporator temperature. Mode of divided molecular still could be used for the separation of mixtures with largely different saturated pressure at one stage operation. Model values agreed well with the experimental values of Cvengros. Maximum relative differences did not exceed 5.1%.

Keywords*:* Binary mixture, Condenser temperature, Feed temperature, Molecular distillation

Introduction

Conventional distillation can not be utilized due to the heat instability of the involved substances, in case of palm oil for obtaining provitamin A, oils of rice for the oryzanol, rice bran wax for octacosanol recovery and natural tocopherols from vegetable oil deodorizer distillate[1-5]. Molecular distillation (MD) appears appropriate for the separation and purification of thermally unstable materials as well as for liquids with low vapor pressure and high molecular weight, without the hazard of thermal decomposition. It is characterized by a short exposure of distilled liquid to elevated temperatures, a high vacuum in the distillation space, and a small distance between the evaporator and condenser[6].

Modeling of MD process includes heat transfer model for the climbing-falling film plate evaporators[7-9]. Lutisan *et al*[10] have developed MD model and investigated the feed temperature with one component, which never represents a real case, assuming the linear temperature profile and the parabolic concentration in film. Cvengros *et al*[8] also investigated fractionation with divided condenser assuming that the condenser and evaporating temperature are constant. Bhandarkar & Ferron[11] as well as Bose & Palmer[12] presented a description of liquid phase transfer processes in high vacuum distillation. Non-ideality of the vapor phase and effect of inert gas pressure have been investigated[13-15]. Simulator DISMOL has been used to determine the evaluation of tocopherol recovery from deodorizer distillate of soya oil and biodiesel from palm oil[1,5].

In this study, a model of MD by using a finite-difference method was brought forward to solve processes in liquid film of the evaporator and the condenser. Effects of feed temperature and condensing temperature on film surface temperature and concentration, evaporation rate, and the degree of evaporation were studied for binary mixtures. Furthermore, divided evaporator and condenser with gradient temperature improve the distillation efficiency and minimize the re-evaporation on the condenser, which is suitable for the separation of mixtures with largely different saturated pressure.

*Author for correspondence
Tel.: +86-551-2901507; Fax: +86-551-2901507
E-mail: Jiangshaotong@yahoo.com.cn

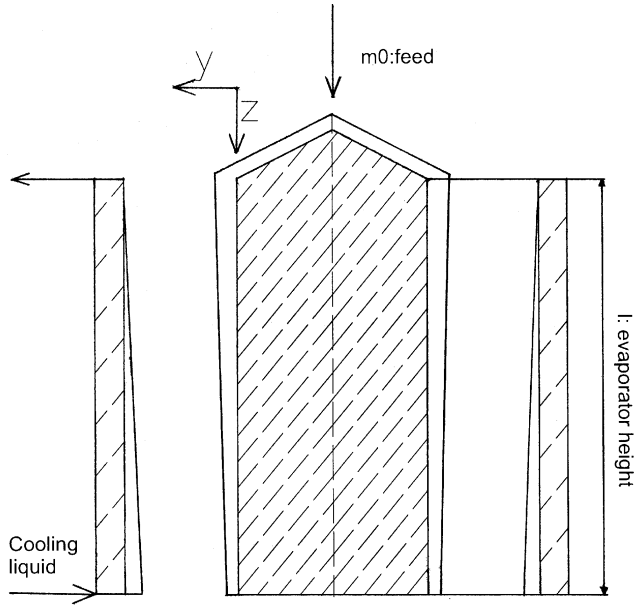

Fig. 1—Scheme of falling film molecular evaporator

Materials and Methods

Mathematical Model of Molecular Distillation

A typical apparatus for the falling film MD (Fig. 1) consists of a cylindrical evaporator surrounded by a condenser jacket. Liquid that is transported through a heater to the evaporation surface flows down in the form of a film and is partly evaporated. Evaporating cylinder is heated internally by the heating fluid at constant temperature (T_{ew}). Condensing cylinder is cooled internally by the cooled fluid at constant temperature (T_{cw}). If both films are thinner than the evaporator and condenser radius, liquid films can be regarded as planar[16]. Inter-molecular collision in the vapor phase is neglected in high vacuum.

Surface Evaporation Rate (High Vacuum)

An expression for the surface evaporation rate of a binary mixture is available from the kinetic theory of gases as follows:

$$G_{ei} = P_{ei}^0 X_{ei}\left(\frac{M_i}{2\pi R_g T_{es}}\right)^{\frac{1}{2}} - P_{ci}^0 X_{ci}\left(\frac{M_i}{2\pi R_g T_{cs}}\right)^{\frac{1}{2}} \quad \ldots (1)$$

$$G_{ci} = -P_{ei}^0 X_{ei}\left(\frac{M_i}{2\pi R_g T_{es}}\right)^{\frac{1}{2}} + P_{ci}^0 X_{ci}\left(\frac{M_i}{2\pi R_g T_{cs}}\right)^{\frac{1}{2}} \quad \ldots (2)$$

where G_{ei} (G_{ci}) is the surface evaporation rate on evaporator (condenser); P_{ei}^0 (P_{ci}^0) is the saturated vapor pressure on evaporator (condenser); M_i is the molecular weight. R_g is the gas constant; T_{es} (T_{cs}) is the surface temperature of the liquid phase on evaporator (condenser); X_{ei} (X_{ci}) is the surface mass concentration of the liquid phase on evaporator (condenser).

Velocity and Thickness Profiles

Velocity profiles for the laminar steady flow of Newtonian fluid in a falling film according to Navier-Stokes equations [16]

$$U_z = \frac{\rho_e g}{\mu_e}\left(y\delta_e - \frac{1}{2}y^2\right) \quad \ldots (3)$$

$$U_y = -\frac{\rho_e g}{\mu e}\frac{y^2}{2}\frac{\mathrm{d}\delta_e}{\mathrm{d}z};\ \frac{\mathrm{d}\delta_e}{\mathrm{d}z} = -\frac{\sum G_{ei}}{C_T}\frac{\mu_e}{\rho_e g \delta_e^{\,2}} \quad \ldots (4)$$

where U_z is axial velocity of the film, ρ_e is density of evaporating film, μ_e is viscosity of evaporating film, y is distance from the evaporator surface, δ_e is evaporating film thickness, U_y is normal velocity of the film derived using continuity equation, C_T is mass concentration of mixture, g is gravitational acceleration, and dz is integration step.

Mass flow and continuity equations for evaporating film give the film thickness:

$$\delta_e = \left[3\mu\left(\frac{m_o}{2\pi R \rho_{\frac{2}{f}} g} - \frac{1}{g\rho_e^2}\int_0^z \sum G_{ei}\right)\right]^{\frac{1}{3}} \quad \ldots (5)$$

where δ_e is evaporating film thickness, ρ_f is density of feed mixtures, and z is axial coordinate of the evaporator.

Temperature Profiles in Liquid Layer

Heat transfer by diffusion in the axial direction will be neglected in comparison with the other two terms because of the liquid flow along axial. Heat transfer is determined by,

$$U_y\frac{\partial T_f}{\partial y} + U_z\frac{\partial T_f}{\partial z} = \frac{\lambda}{\rho C_p}\frac{\partial^2 T_f}{\partial y^2} \quad \ldots (6)$$

where C_p is thermal capacity, T_f is temperature of film, and λ is thermal conductivity. Initial and boundary conditions are: $z = 0, 0 \le y \le \delta$, $T = T_f$ (evaporating film)

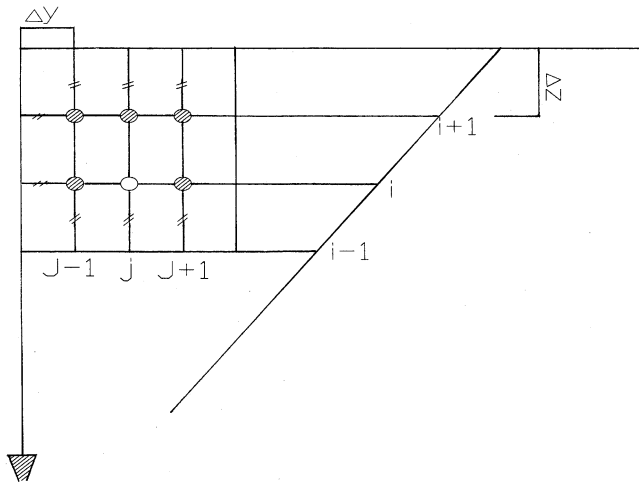

Fig. 2—Scheme of the Crank-Nicholson net of evaporating film

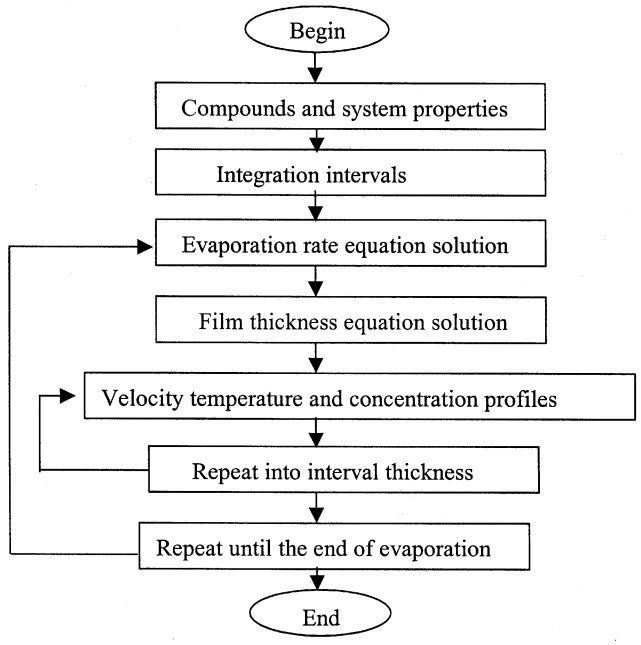

Fig. 3—Simulation procedure of molecular distillation model

$$y=0,\ \ T=T_w,\ \ \ y=\delta,\ \ \lambda\frac{\partial T_f}{\partial y}=-\sum_{i=1}^{2}R_{avi}G_i$$

where T_f is feed temperature, T_w is wall temperature, and R_{avi} is evaporation enthalpy.

Concentration Profiles in Liquid Layer

Concentration profiles in the liquid layer for a multicomponent mixture can be expressed by Eq. (7), which is valid for negligible axial diffusion.

$$U_y\frac{\partial C_f}{\partial y}+U_z\frac{\partial C_f}{\partial z}=D\frac{\partial^2 C_f}{\partial y^2} \qquad \ldots (7)$$

where D is mass diffusion coefficient, which is to be held constant, and C_f is concentration of film. Initial and boundary conditions are

$$z=0,\ 0\le y\le\delta,\ \ C=C_f,\ \ y=0,\ \ T=T_w,$$

$$\frac{\partial C_f}{\partial y}=0;\ \ y=\delta,\ \ D\frac{\partial C_f}{\partial y}=-\frac{-\left(G_i-X_i\sum_{j=1}^{2}G_j\right)}{\rho}$$

where C_f is feed concentration, and T_w is wall temperature.

The equations describing diffusion and thermal balance are modified to a convenient form to apply the finite differences method and solved by an implicit finite differences method[17]. In this study, the stable Crank-Nicholson scheme was used for the transformation of partial differential equation into discrete form. Film thickness was divided in 100 equal intervals, and evaporation length, L, was divided into 300 equal intervals. For each value of z, value of y will vary with integration step. Temperature and concentration in the node i, j were calculated from the set of equations (Fig. 2). So, the system of equations is solved as

$$\frac{T_i^j-T_{i-1}^j}{\Delta z}=\frac{1}{2}\frac{\lambda}{\rho C_p}\left(\frac{T_i^{j+1}-2T_i^j+T_i^{j-1}}{\Delta y^2}+\frac{T_{i-1}^{j+1}-2T_{i-1}^j+T_{i-1}^{j-1}}{\Delta y^2}\right) \qquad \ldots (8)$$

$$\frac{C_i^j-C_{i-1}^j}{\Delta z}=\frac{1}{2}D\left(\frac{C_i^{j+1}-2C_i^j+C_i^{j-1}}{\Delta y^2}+\frac{C_{i-1}^{j+1}-2T_{i-1}^j+T_{i-1}^{j-1}}{\Delta y^2}\right) \qquad \ldots (9)$$

$$\frac{T_i^{j_{\max}}-T_i^{j_{\max-1}}}{\Delta y}=-\frac{R_{avi}G_i}{\lambda};$$

$$\frac{C_i^{j_{\max}}-C_i^{j_{\max-1}}}{\Delta y}=-\frac{-\left(G_i-X_i\sum_{j=1}^{2}G_j\right)}{\rho_1 D} \qquad \ldots (10)$$

Computational scheme for the model proceeds is shown in Fig. 3. Mathematical method is highly stable and results were convergent after using sufficiently

reduced integration step. Calculation programs were developed and debugged using Matlab® software Version: 6.5 (The MathWorks, Inc. Boston, MA, USA).

Results and Discussion

A binary mixture of esters [di-butyl-phthalate (DBP, M = 278.3 g mol^{-1}) and di-butyl-sebacate (DBS, M = 314.5 g mol^{-1})][18,19] tested separating efficiency of evaporator. Other parameters are: mass diffusion coefficient, 1.0×10^{-8} m^2 s^{-1}; pressure considered, 0.10 Pa; distance from evaporation surface to condenser surface, 0.0185 m; evaporation heated surface length, 0.6000 m; condenser length, 0.6000 m; inside evaporator diam, 0.0550 m and condenser diam, 0.0180 mm. In the case of divided condenser and divided evaporator, it was separated into three zones (height, 0.2000 m) or it was separated into two zones(height, 0.3000 m). If divided evaporator and condenser are applied, individual zones temperature of evaporator and condenser could be controlled separately and individual distillate from zones on the condenser could be collected separately.

Influence of Feed Temperature

For various feed temperatures (293, 313, 333, 353 and 363 K), film thickness at $z = 0$ is given by Eq. (5) in Nusselt's approximation. Film thickness decreases when feed temperature increases, due to temperature dependence of viscosity and evaporation (Fig. 4A). Thickness of evaporating film is almost linear to axial direction, which is similar to the results of Ruckenstein & Hassink[20] and largely different from parabolic shape developed by Cvengros *et al*[8] simulated with one component model, which did not existed in real case. As feed temperature increased, evaporating film surface concentration decreased sharply because of evaporation (Fig. 4B). At high values of T_f, large heat and mass transfer takes place. When feed temperature is 363 K, surface concentration at 0.6 m decreased (37.25%).

Feed temperature has the same asymptotic temperature of film surface, which is little below than evaporator temperature (Fig. 4C). For example, when feed temperature is 293 K, the evaporator's end film surface temperature is 355 K and do not reach a steady state. The length of evaporating cylinder along with the surface temperature of evaporating film reaching a steady-state decreases with increasing feed temperature because of the relatively low thermal diffusion of two components mixture and change of film surface concentration in this model. Thus, the feed temperature has large importance on MD.

Dependence of evaporation rate, degree of evaporation and concentration of distillate upon the axial direction is shown in Figs 4D, 4E and 4F, respectively. Evaporation rate ($z = 0$) is calculated by Eq. (1) at feed concentration and feed temperature, which is different to the results of Batistella & Maciel[21] with the assumption that the feed temperature is at the distillation temperature. With the increase of feed temperature, evaporation rate increases due to the increase of surface temperature (Fig. 4C). However, evaporation rate decrease takes place gently in the later part of the evaporator especially for higher feed temperature. There, it could be explained by Eq. (1) that the surface concentration (Fig. 4B) has dominating influence on evaporation rate whereas the surface temperature nearly stays constant at the latter part of the evaporator (Fig. 4C). The degree of evaporation, expressed as a ratio of the distillate weight to the feed, D_w/F, increases monotonically, almost linearly with z especially for higher feed temperature, except for T_f = 313 K (Fig. 4E). Higher evaporator temperature increases D_w/F value, and decreases concentration of distillate for all z (Fig. 4F), which is connected with an increase of the evaporation rate with the increase of T_f and the less volatile DBS is also evaporated more and more (Fig. 4D). This effect can be explained that for attaining an equal degree of distillation is necessary, at some evaporator temperature, to raise feed temperature. On the other hand, higher feed temperature is accompanied with a decreased concentration of more volatile component. Therefore, there appears to be a compromise between the maximum degree of evaporation and desired concentration of component. One condensate is obtained by the undivided molecular still. If splashing occurs, the quality of condensate is poorer. Moreover, operating parameters are difficultly adjusted to obtain desired concentration of distillate in one stage operation of MD.

Influence of Condensing Temperature

Thickness of condensing film increases along the axial direction, mainly due to the gravitational force (Fig. 5A). Film thickness decreases with increase of condensing temperature, due to low viscosity and evaporation leading to the decrease in the amount of liquid on the condenser at high condensing temperature. Surface temperature of condensing film

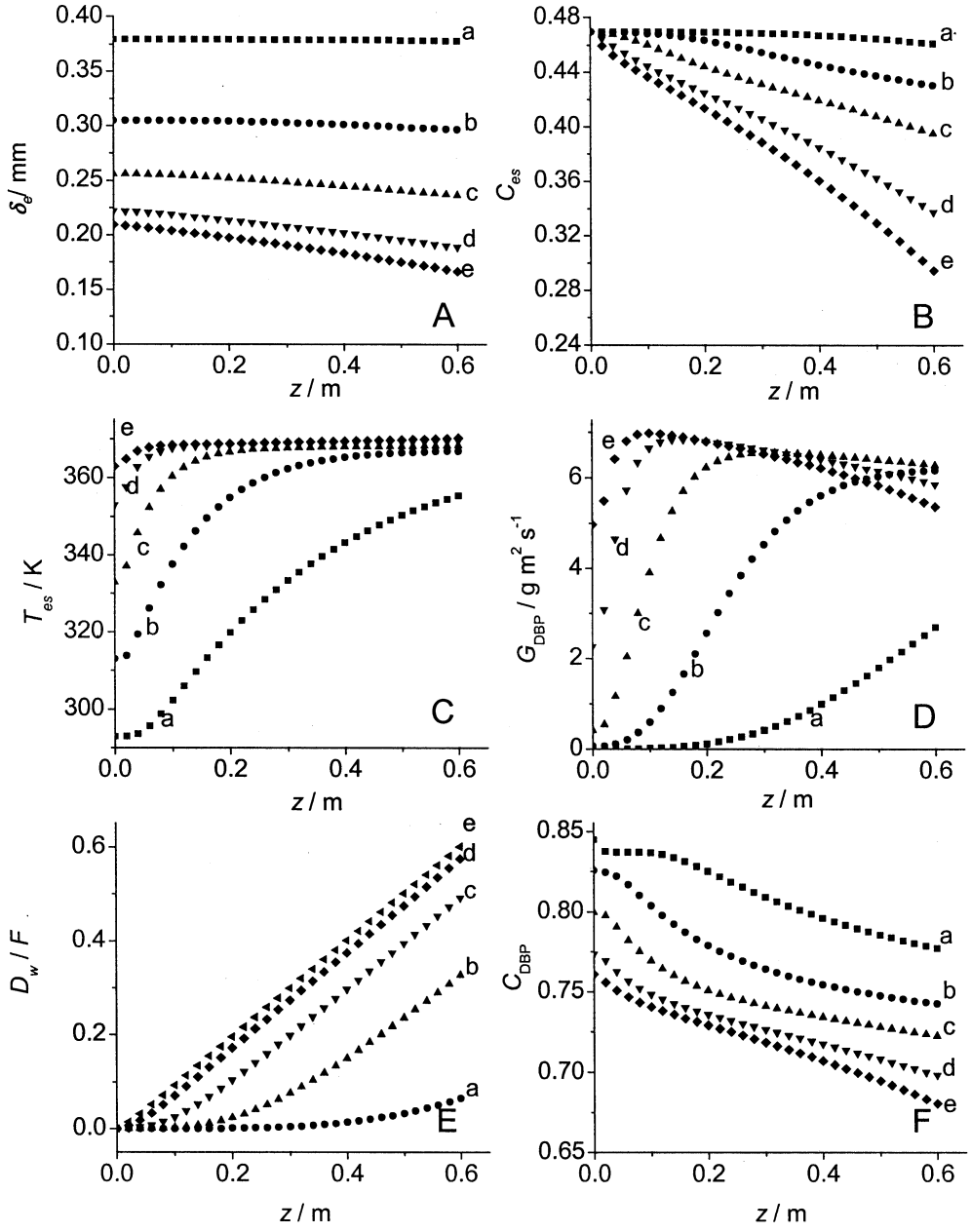

Fig. 4—Position dependence of: A) Evaporating film thickness; B) Evaporating film surface concentration (ratio) of DBP; C) Evaporating film surface temperature; D) Evaporation rate; E) Degree of evaporation; F) Concentration (ratio) of distillate for different feed temperatures (T_f): a, 293 K; b, 313 K; c, 333 K; d, 353 K; and e, 363K (T_{ew} = 373 K, T_{cw} = 273 K, m_o = 1.6 g s^{-1})

increases along the axial coordinate (Fig. 5B). Temperature of the condenser surface layer is higher than that of the cooling medium, preventing total irreversible condensation of molecules and causing a partial re-evaporation from condenser lowering the separatory power of the process. So, for T_{cw} of 273 K, temperature difference T_{cw} and T_{cs} at the end of condenser is about 13 K, which corresponds, at a film thickness of about 0.5 mm, to a gradient as high as 26 K mm^{-1}. Concentration of more volatile component (DBP) decreases obviously when the condensing temperature is above 313 K corresponding to the change of evaporating rate because of the re-evaporation of molecules on the condenser (Figs 5C & 5D). The concentration of distillate and degree of evaporation decreases obviously with higher condensing temperature because of the re-evaporation with the exception of T_{cw} of 273, 293 and 313 K

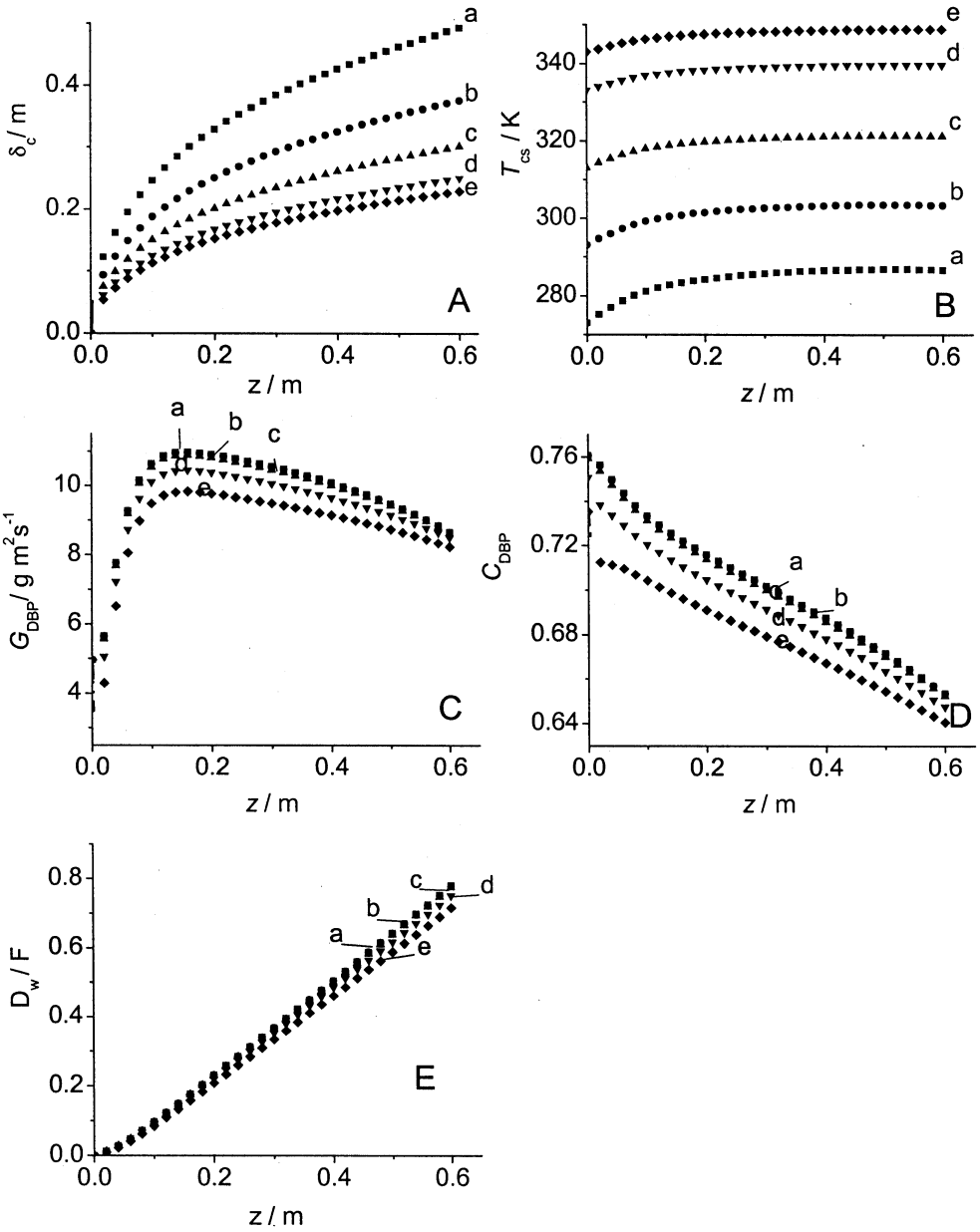

Fig. 5—Position dependence of: A) Condensing film thickness; B) Condensing film surface temperature; C) Evaporation rate; D) Concentration of distillate; E) Degree of evaporation for different condenser temperatures (T_{cw}): a, 273 K; b, 293 K; c, 313 K; d, 333 K; and e, 343K (T_{ew} = 383 K, T_f = 363 K, m_o = 2.0 g s^{-1})

(Figs 5D & 5E). Therefore, in one stage of MD, less condensing temperature, which is a little higher than the melting point of distillate to ensure the flow of distillate, is preferred aiming to minimize of re-evaporation. However, constant condensing temperature and evaporation temperature are not suitable for the separation of multicomponent, which has largely different physical parameters in one stage process. When the separation efficiency of one stage operation is not sufficient, operation is repeated, such as the tandem of apparatuses could be used, but repeat operation makes the process labor-intensive, time-consuming and of high cost. For instance, fatty acid methyl ester, tocopherol and sterol ester in the vegetable oil deodorizer distillate couldn't be separated at high production efficiency in one stage. So, divided evaporator and condenser were suggested to intensify the MD process and provide approach for the process design and development.

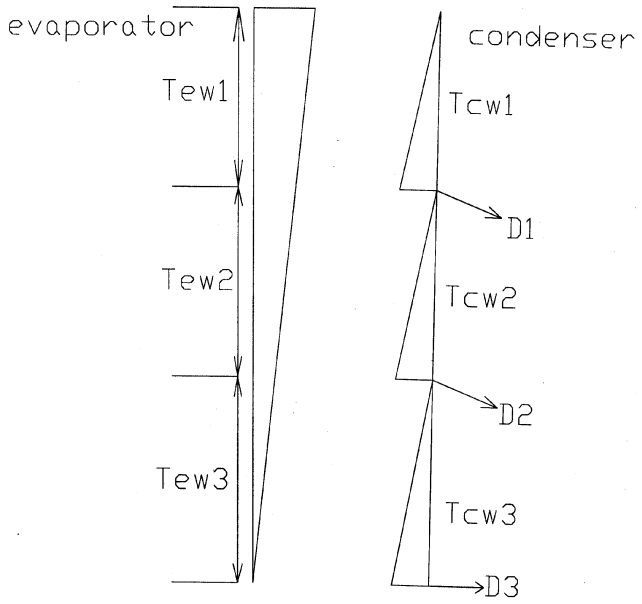

Fig. 6—Molecular still with divided evaporator and divided condenser

Influence of Divided Evaporator and Condenser

Fractionation or collection of fractions of different content of the more volatile component is significantly restricted, and multicomponent is difficult to be separated when using a one-stage molecular evaporator in the practical production. Therefore, divided evaporator and condenser were suggested (Fig. 6). It is assumed that molecules evaporate from the evaporating cylinder of some temperature at a certain height and also condense predominantly at the same height of the closely positioned condenser.

The divided condenser, due to a smaller thickness of the condensed films than in the case of the undivided one, shows lower surface temperature of condensing film, heightening total irreversible condensation of molecular (Fig. 7A). For three condensers, the condenser film surface temperature of 278 K at $z = 0$ is lower than 280 K of the undivided condenser. Similar result is reported by Cvengros *et al*[8]. Fig. 7B demonstrated the development of condensing film surface

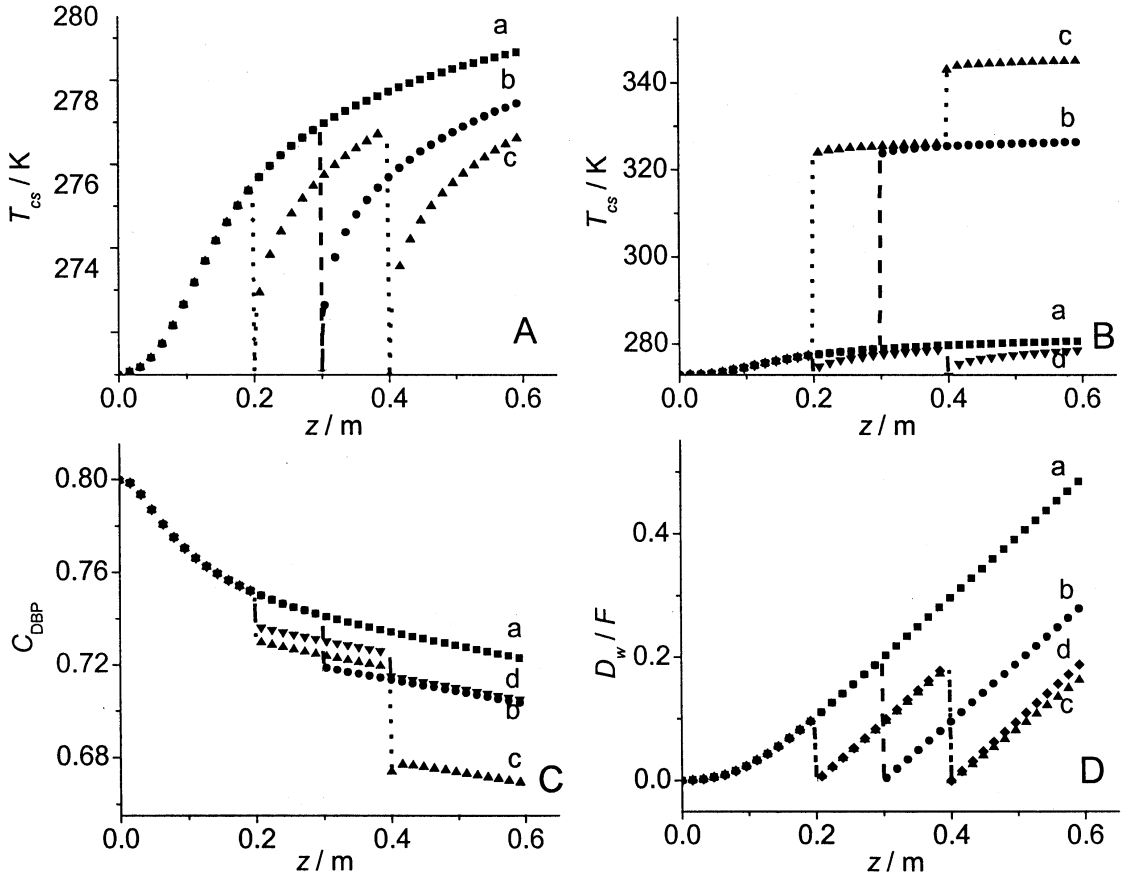

Fig. 7—Position dependence of: A) Condensing film surface temperature at constant condenser temperature; B) Condensing film surface temperature at gradient condenser temperature; C) Concentration of distillate; D) Degree of evaporation for divided condenser For A: a, T_{cw}=273 K; b, T_{cw1}=T_{cw2}=273 K; and c, T_{cw1}=T_{cw2}=T_{cw3}=273 K. For B, C and D: a, T_{cw}=273 K; b, T_{cw1}=273 K, T_{cw2}=323 K; and c, T_{cw1}=273 K, T_{cw2}=323 K, T_{cw3}=343 K, T_{cw1}=T_{cw2}=T_{cw3}=273 K, T_{ew} = 373 K, T_f = 333 K, m_o = 1.6 g s^{-1}

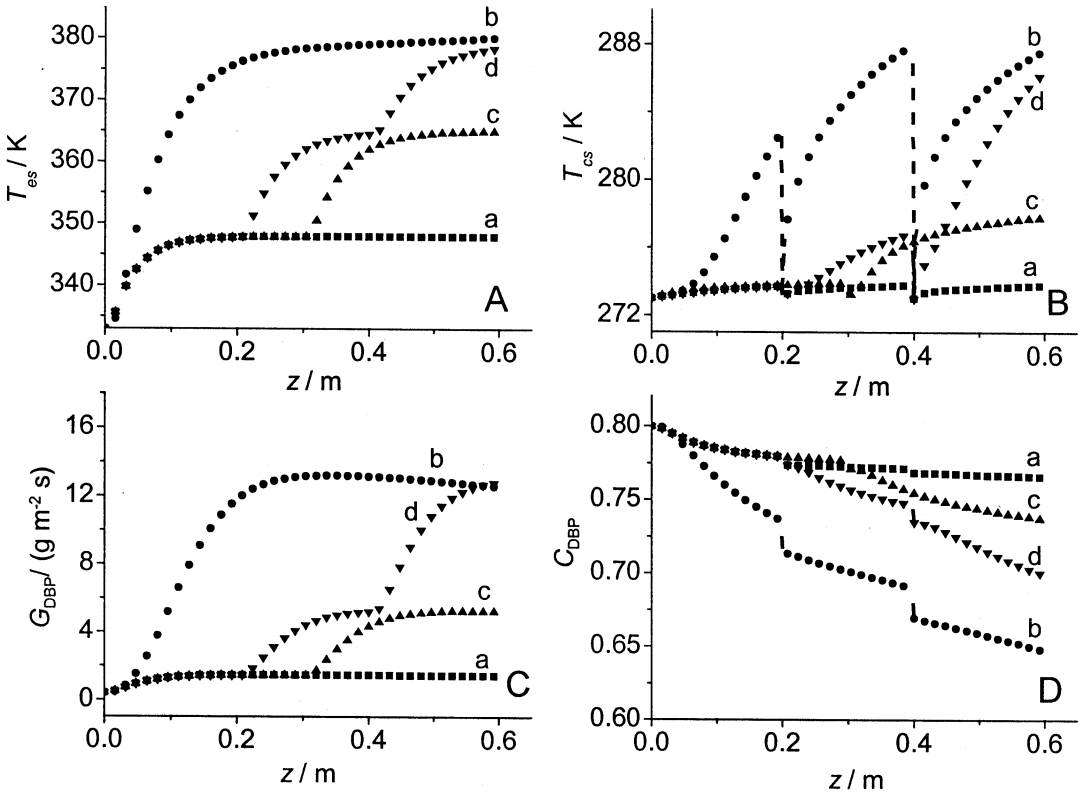

Fig. 8—Influence of gradient evaporator temperature on: A) Evaporation film surface temperature; B) Condensing film surface temperature; C) Evaporation rate; D) Concentration of distillate for divided evaporator and three condensers. For A-D: a, T_{ew}=349 K; b, T_{ew}=389 K; c, T_{ew1}=349 K, T_{ew2}=369 K; and d, T_{ew1}=349 K, T_{ew2}=369 K, T_{ew3}=389 K, T_f = 333 K, T_{cw} = 273 K, m_o = 1.6 g s^{-1}

temperature along the condenser height. Sharp increase of temperature takes place at the transition from one zone to another with the gradient increase of individual condenser temperature. The lower and higher melting point substances could be separated and flows smoothly. It is suitable for the treatment of mixtures with largely different melting point substances in one stage operation.

In MD with binary mixtures, largely gradient concentration of desired component is obtained than undivided condenser due to re-evaporation in the latter condenser parts (Fig. 7C). If the distillate content of 0.70 is preferred, the latter condenser temperature could be adjusted to satisfy desired content. Passing from one section of condenser to another cause discontinuous changes in the distillate composition, which is the consequence of draining off cumulated distillate and by commencing the collection of new one. Influence of gradient T_{cw} on total degree of evaporation for divided condenser is not obvious and increases monotonically, almost linearly with z especially for the latter condenser zones (Fig. 7D).

Three gradient evaporator temperatures (349, 369 and 389 K) were selected for divided evaporator and three condensers. Evaporating film surface temperature increases from feed temperature (333 K) to a steady state near to the first zone temperature at the connecting of zones, and then increases to the latter zone temperature (Fig. 8A). So, divided evaporator is suitable to separate the largely different saturated pressure of substances in the food industry. For instance, fatty acid methyl esters, tocopherol and sterol esters may be separated at one stage operation. The gradient evaporator temperature also influences surface temperature of the film on condenser, which is connected with large transfer of evaporation enthalpy at higher temperature of the evaporator, causing the increase of the condenser film surface temperature (Fig. 8B). The decrease tendency of evaporation rate at the latter part of the evaporator at constant evaporator and condenser temperature is restricted by the divided evaporator because of the temperature of evaporating film surface always has dominating influence (Fig. 8C). Any desired concentration of DBP could be derived by adjusting the divided evaporator

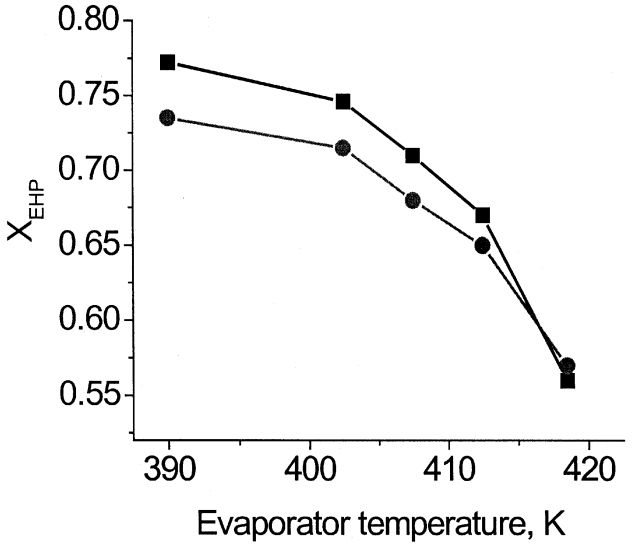

Fig. 9—Comparison between theoretical model (■) and results of Cvengros *et al*[8] (●)

temperature and condenser temperature (Fig. 8D). The proposed model with divided still enables the simulation of multicomponent systems. However, in this study, only two components are considered because the main objective is to consider the influence of feed and condenser temperature for divided condenser and evaporator.

Comparison between Theoretical Model and Experimental Results

MD study can be compared with experimental data[8] on a mixture of di-(2-ethyl hexyl) phthalate (EHP; M = 391 g mol^{-1}) with di-(2-ethyl hexyl) sebacate (EHS; M = 426 g mol^{-1}) in molar ratio 1:1. Physical properties used in these computations were from reported studies[8,10,12]. Effect of collisions in the distillation gap is presumed negligible. Modeled molecular evaporator has a 30 mm-diam evaporator cylinder (295 mm height), which is same as the reported[8] one. Representative values of some variables were as follows: feed rate, 950 g h^{-1}; feed temperature, 343 K; and mass diffusivity, 10^{-8} m^2 s^{-1}. The models values agree well with the reported values[8] (Fig. 9). The maximum relative error does not exceed 5.1%. May be it is mainly connected with negligence of the intermolecular collision in the distillation space in the model and assumption of laminar layers which is partly existed in the fluid.

Conclusions

Balanced equations of a binary mixture for molecular distillation were derived on the basis of relation of heat and mass transfer in liquid films on both the evaporating and condensing surface. The length of evaporating cylinder along with the surface temperature of evaporating film reached steady state decreasing with increasing feed temperature. Evaporation rate decreased with increasing condensing temperature because of the re-evaporation. Divided condenser minimized influence of splashing on distillate and increased degree of evaporation of gradient concentration of desired substance. Evaporating film temperature gradient increased with the gradient temperature of divided evaporator. The separation of mixtures with largely different saturated pressure could be fulfilled and desired concentration of distillate could be obtained by the divided evaporator. Finally, the model values agree well with the reported values[8]. Maximum relative error does not exceed 5.1%. It was advantageous and effective for feeding pre-heating material to temperatures close to steady state and decreasing condensing temperature.

Acknowledgements

Authors thank Natural Science Foundation of Anhui Province, China (Project No. 03041302) for financial support. Authors also gratefully acknowledge the contribution of Prof. Y Y Zhao for his valuable advice.

References

1 Batistella C B, Moraes E B, Maciel F R & Wolf M M R, Molecular distillation process for recovering biodiesel and carotenoids from palm oil, *Appl Biochem Biotechnol,* **98** (2002) 1149-1159.

2 Chen F, Cai T Y, Zhao Y H, Liao X J, Guo L Y & Hu X S, Optimizing conditions for crude octacosanol extract from rice bran wax by molecular distillation analyzed using response surface methodology, *J Food Engg*, **70** (2005) 47-53.

3 Ghosh S & Bhattacharyya D K, Isolation of tocopherol and sterol concentrate from sunflower oil deodorizer distillate, *J Am Oil Chem Soc*, **73** (1996) 1271-1274.

4 Nongluk C, Supaporn C, Peter D & Wilai L, Simulation of an agitated thin film evaporator for concentrating orange juice AspenPlus™, *J Food Engg,* **47** (2001) 247-253.

5 Moraes E B, Batistella C B, Torres A M E, Maciel F R & Wolf M M R, Evaluation of tocopherol recovery through simulation of molecular distillation process, *Appl Biochem Biotechnol,* **113** (2004) 689-710.

6 Burrows G, *Molecular Distillation* (Oxford University Press, London) 1960, 21-25.

7 Ribeiro Jr C P & Cano A M H, A heat transfer model for the steady-state simulation of climbing-falling-film plate evaporators, *J Food Engg*, **54** (2002) 309-320.

8 Cvengros J, Lutisan J & Mirov M, Feed temperature

influence on the efficiency of a molecular evaporator, *Chem Engg J*, **78** (2000) 61-67.

9 Cvengros J, Mirov M & Lutisan J, Modeling of fractionation in a molecular evaporator with divided condenser, *Chem Eng Process*, **39** (2000) 191-199.

10 Lutisan J, Cvengros J & Mirov M, Heat and mass transfer in the evaporating film of a molecular evaporator, *Chem Engg J*, **85** (2002) 225-234.

11 Bhandarkar M & Ferron J R, Transport processes in thin liquid films during high-vacuum distillation, *Ind Eng Chem Res*, **27** (1988) 1016-1024.

12 Bose A & Palmer H J, Influence of heat and mass transfer resistances on the separation efficiency in molecular distillations, *Ind Eng Chem Fundam*, **23** (1984) 459-465.

13 Lutisan J & Cvengros J, Effect of inert gas pressure on the molecular distillation process, *Sep Sci Technol*, **30** (1995) 3375-3389.

14 Batistella C B, Maciel M R W & Maciel F R, Rigorous modeling and simulation of molecular distillators: Development of a simulator under conditions of non-ideality of the vapor phase, *Comp Chem Eng*, **24** (2000) 1309-1315.

15 Zhang X B, Xu C J & Zhou M, Simulation of molecular distillation between coaxial cylinder at high vacuum, *Chin J Process Engg*, **5** (2005) 97-102.

16 Levenspiel O, *Chemical Reaction Engineering* (John Wiley & Sons, New York) 1972, 253-278.

17 Fletcher J A C, *Computational Techniques for Fluid Dynamics*, **2nd edn** (Springer, Berlin) 1991, 14-19.

18 Kawala Z, A dibutyl phthalate-dibutyl sebacate mixture as a system for testing molecular distillation column, *Int Chem Engg*, **14** (1974) 536-543.

19 Yaws C L, *Chemical Properties Handbook* (McGraw-Hill, New York) 1999, 178-179.

20 Ruckenstein E & Hassink W J, The combined effect of diffusion and evaporation on the molecular distillation of ideal binary mixture, *Sep Sci Technol*, **18** (1983) 523-545.

21 Batistella C B & Maciel M R W, Modeling, simulation and analysis of molecular distillators: Centrifugal and falling film, *Comp Chem Eng*, **20 (suppl)** (1996) 19-24.